Qlassifier: Miniatured Hybrid Quantum-Classical Convolutional Neural Network

Dongok Kim
Department of Physics
Korea Advanced Institute of Science and Technology
Daejeon, Republic of Korea
physicist@kaist.ac.kr

BoSeong Kim
Department of Physics
Yonsei University
Seoul, Republic of Korea
boseong14@gmail.com

Yunseo Kim
Department of Physics and Astronomy
Seoul National University
Seoul, Republic of Korea
yunseo47@protonmail.ch

Hojun Lee
School of Electrical Engineering
Korea Advanced Institute of Science and Technology
Daejeon, Republic of Korea
quantum0430@kaist.ac.kr

Jaehoon Hahm
Department of Physics and Astronomy
Seoul National University
Seoul, Republic of Korea
judol1@snu.ac.kr

Abstract

Our model applies quantum convolution filters - quanvolution filters - to get nonlinear feature maps. Since research in machine learning algorithms showed that such nonlinearity could increase accuracy or decrease training times, we can expect some quantum advantage to feature such nonlinear characteristics of the data. However, It is not shown in the previous research that such benefit originates in its quantum feature. Therefore we will first carefully construct the quanvolutional neural network proposed from former research. And then, choosing certain circuits of the quanvolutional layer and varying methods applied in the layer, we will figure out if there could exist a quantum feature in the classical dataset that significantly benefits the accuracy or efficiency of the model.

1 Introduction

A concept of the quantum computer had been proposed to compute and simulate the nature in natural way in early 1980s Benioff (1980); Feynman (1982); Manin (1980). The reversible quantum logic gates (NOT, Controlled NOT (or CNOT), and Controlled Controlled NOT) were also motivated by the time reversibility of the laws of quantum physics Feynman (1985); Toffoli (1981). The quantum computer employs quantum computations, so it is expected to be more proper for simulating and evaluating the natural phenomena rather than a classical computer. Recent works claimed their quantum computations will not be reprogrammed by any classical computers in any feasible amount of time, or achievement of the *quantum supremacy* Arute et al. (2019); Zhong et al. (2020); Wu et al. (2021).

One of the most interesting and important computer algorithms in this era is the machine learning Goodfellow et al. (2016). After the legendary Baduk (Go) games of AlphaGo and AlphaGo

Preprint.

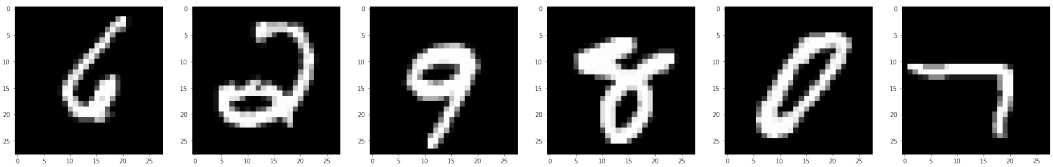

Figure 1: 6 MNIST data from training dataset representing the Arabi numerals 6, 2, 9, 8, 0, and 7.

Zero played with Sedol Lee and other top-tier Baduk players, the machine learning became more popular among not only computer science researchers, but also the general public Silver et al. (2016, 2017). Both AlphaGo and AlphaGo Zero were designed based on the deep learning built on a neural network, which extracts a pattern from given data. The (deep) neural network is now the standard of the (deep) machine learning model.

Deep machine learning models over successful applications faces a new challenge that whether it can extract any patterns from *quantum data*, or on the other front, whether the deep machine learning model can be built on the *quantum computer* (See Refs. for reviews Biamonte et al. (2017); McArdle et al. (2020)). There have been enormous investigations of the machine learning using either quantum data or quantum processor, especially for a classification of images based on convolutional neural networks (CNNs) Cong et al. (2019); Henderson et al. (2019); Kerenidis et al. (2020); Kerenidis and Luongo (2020); Oh et al. (2020); Pesah et al. (2020); Chen et al. (2020); Wei et al. (2021); Liu et al. (2021).

In this report, we present a quick quantum algorithm for classifying image datasets based on the hybrid quantum-classical convolutional neural network (HQC CNN) to demonstrate the quantum advantage can be realized under small sizes of datasets, small number of quantum bits (qubits), and small number of training iteration steps. We show that in this miniatured model get similar result from the Ref. Henderson et al. (2019) with appropriate qubit encoding method. We also designed various quantum circuits (QCs) for HQC CNN to figure out effect of quantum circuit characteristics suggested in Ref. Sim et al. (2019), and compare a classification performance of those quantum circuits in terms of classification accuracy.

2 Background

2.1 Image dataset

The MNIST dataset is consisting of 70,000 handwritten Arabic numerals, and widely used for classification models in the machine learning field. 60,000 of them are used to train the classification model, and left 10,000 of them are used to test (validation dataset) the model. Each of data is a grayscale image of 28 by 28 pixels, and a single pixel has a value from 0 to 255 (8-bit). Figure 1 represents 6 MNIST data of Arabic numerals 6, 2, 9, 8, 0, and 7. Conventionally, the value range $[0, 255]$ is normalized to the unit interval $[0, 1]$.

Since a background and the characteristic feature are colored as black and white, respectively, a performance of a classifier is determined by how it is strong to distinguish the darkest and the brightest patterns by evaluating correlations for given image data. Figure 2 shows histograms of the normalized values for randomly selected 100 MNIST images from training and test datasets. Note that Fig. 2 is represented in the logarithm scale and the most of gray pixels do not contribute to the image. Which means this binary characteristic could generate an interesting feature by controlled gates in a QC.

2.2 Classical convolutional neural network

A CNN is a one of deep neural network based on weighted convolution of a neural network layer and kernel or filter. It has been widely used in the image (2D) or video (3D) pattern analyses such as classification or object detection, respectively. The convolution have infinitely many combinations when it transfers information (or feature) between two neighboring layers. Therefore, there exists a trade-off between the number of operations and degree of freedom.

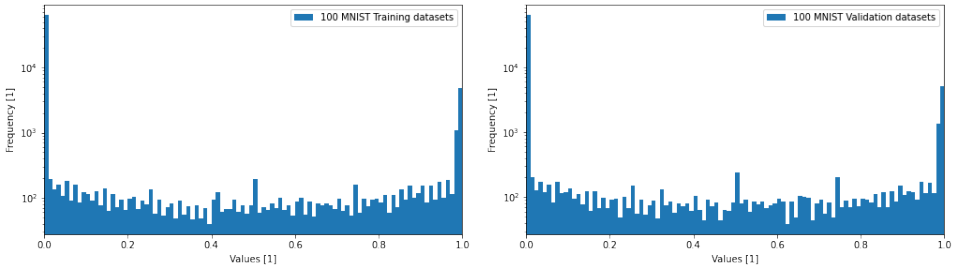

Figure 2: A histogram of the MNIST dataset pixels. 100 random samples from both training (left) and validation (right) datasets are used. The total number of pixels for each histogram is $100 \times 28 \times 28 = 78,400$.

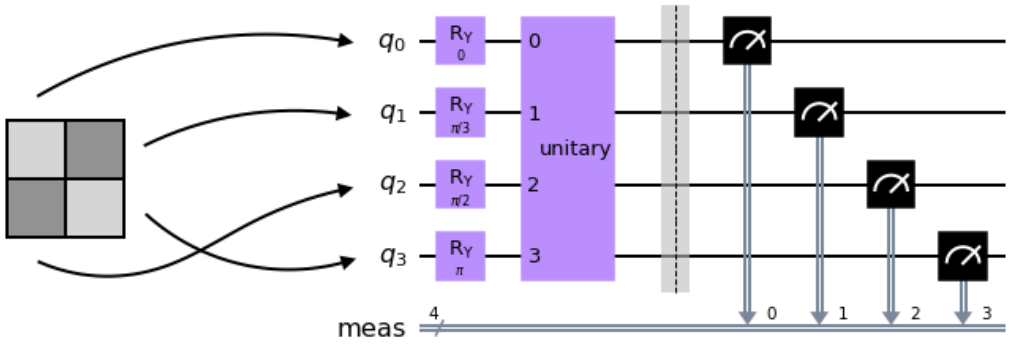

Figure 3: An example of the quantum circuit for 4 pixels. The initialization angles for each encoded qubit are chosen arbitrarily.

2.3 Quantum circuit and quantum bit encoding

The normalized pixel data are needed to be encoded to qubit state. The number of qubits in a quantum computer determines the maximal kernel size, and the entangled pair configuration plays a key role to compose a QC with multiple-qubit gates under less CNOT-cost.

Each pixel can have a value between the darkest to the brightest values ranged in $[0, 1]$. Without lose of generality, it can be mapped by the encoding function e as

$$e(0) = |0\rangle, \quad e(1) = |1\rangle. \tag{1}$$

The intermediate value can be represented by an angle rotated along any axes in the xy-plain. Let the axis be y-axis. Then the qubit state corresponding to the normalized value v is

$$e(v) = R_y\left(v\pi\right)|0\rangle, \tag{2}$$

where $R_y(\theta)$ is the rotation gate along the y-axis with an angle θ.

The encoded data will pass through a QC as shown in the Figure 3. The number of pixels used in the QC can be different depending on the number of available qubits in the quantum simulator or quantum computer.

2.4 Quantum convolutional layers

As described in the previous subsection, the quantum convolutional layer should consider a computing cost, which is relevant to the number of two-qubit gates in a QC. Those quantum (unitary) operations will be conducted right after the data values are encoded to the qubit states as shown in the Fig. 3.

The classification performance can be different for different parametrized quantum circuits (PQCs). These PQCs are characterized by expressibility and entangling capability; the expressibility represents

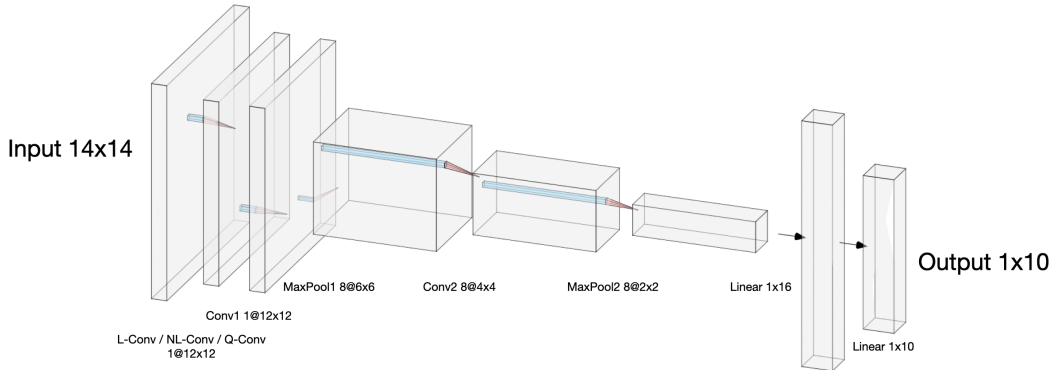

Figure 4: The neural network architecture used in the hybrid quantum-quantum convolutional neural network model.

how well the Hilbert space is constructed and the entangling capability represents a quantified ability to generate entangled states for given QC Sim et al. (2019). Both of them are important in the degree of freedom (expressibility) and the number of operations (entangling capability).

3 Method

The MNIST dataset is used to evaluate both pure-classical and hybrid quantum-classical convolutional neural network models. To reduce the computing cost, the MNIST dataset are resized to 14 by 14 pixels in advance. The MNIST datasets are randomly sampled for 50 training and 30 validation datasets without shuffling, but with random sampler under fixed random seed or 47. The batch size of training is 10 and the number of epochs is set to 10.

The overall structure of the convolutional neural network is illustrated in the Figure 4. The first convolutional layer is a core of this research. Three different types of layer are applied; L-Conv (CNN), NL-Conv (NL-CNN), and Q-Conv (QNN). L-Conv indicates the linear convolutional layer with the 3 by 3 kernel. NL-Conv indicates the non-linear convolutional layer with the same kernel size, but at most 4th polynomial map is applied. Finally, Q-Conv has a quantum convolutional layer with encoding map in Eq. 2 with various PQCs. The expectation value of σ_z (Pauli matrix) of the 1st qubit is used as a decoded value.

Four PQCs are designed based on the previous work for 4-qubit PQC Sim et al. (2019). We extended 4-qubit PQCs to 9-qubit PQCs and evaluated QC characteristics. Each PQC is drawn in the Figure 6 in the A. Table 1 lists the characteristic of distinct PQCs. The expressibility is estimated by a Kullback-Leibler divergence from fidelity histogram of 5,000 samples and 1,000 bins. The entangling capability is evaluated by the Meyer-Wallach measure with 100 samples Meyer and Wallach (2002).

The left structure after L-Conv, NL-Conv, and Q-Conv is common: CONV1 - POOL1 - CONV2 - POOL2 - FC1 - DROPOUT - FC2. The number of channels through convolutional layers is 8, and the kernel size of two convolutional layers is same as before, 3 by 3. Two pooling layers use the maximul value with 2 by 2 kernel. The first full-connected layer has a length of 16 data, and the second one has 10 outputs. The dropout has a probability of 0.4. The ADAM optimization is used with the learning rate 0.03 Kingma and Ba (2014).

Due to lack of time, only QNN-9 is compared under limited number of trainings.

4 Result and Conclusion

The training result is shown as in the Figure 5. Even their accuracy shows low values, however the loss is reduced with respect to the epochs. The accuracy and loss are listed as well in the Table 2.

Even though this miniatured hybrid quantum-classical convolutional neural network does not analyze full features of the variety of quantum convolutional neural network, it showed the quantum advantage under small sizes of datasets, small number of quantum bits (qubits), andsmall number of training

Table 1: Characteristics of quantum circuits used in the hybrid quantum-quantum convolutional neural network models. Expressibility, entanglement capability, number of parameters, and the number of two qubit gates (CNOT cost) are listed for each quantum circuit.

Models	Expressibility	Entangling cap.	# parameters	CNOT cost
QNN-2	0.34	0.80	18	8
QNN-3	0.30	0.17	26	8
QNN-9	0.27	1.00	9	8
QNN-10	0.31	0.37	18	9

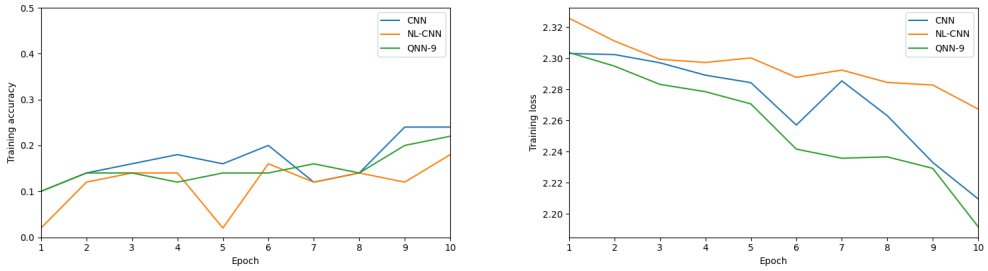

Figure 5: The training accuracy and loss with respect to the epochs for three models, CNN, NL-CNN, and QNN-9.

iteration steps. It provides a future opportunity to general public to approach quantum machine learning even in the limited computing resource environment.

Acknowledgments and Disclosure of Funding

The authors are greatful to Daniel K. Park, Junki Kim, and all other mentors for helpful insights and discussions. The authors also thank to IBM, IonQ, and all other organizers for holding 2021 Quantum Hackaton Korea.

References

P. Benioff, Journal of Statistical Physics **22**, 563 (1980).

R. P. Feynman, International Journal of Theoretical Physics **21**, 467 (1982).

Y. Manin, Russian. Partial English translation in [Man99] (1980).

R. P. Feynman, Optics News **11**, 11 (1985).

T. Toffoli, Mathematical systems theory **14**, 13 (1981).

F. Arute, K. Arya, R. Babbush, D. Bacon, J. C. Bardin, R. Barends, R. Biswas, S. Boixo, F. G. S. L. Brandao, D. A. Buell, et al., Nature **574**, 505 (2019).

Table 2: The performance comparison among neural network models at 10 epochs for MNIST dataset

Models	Training accuracy (%)	Training loss
CNN	24	2.21
NL-CNN	18	2.26
QNN-2	-	-
QNN-3	-	-
QNN-9	22	2.19
QNN-10	-	-

H.-S. Zhong, H. Wang, Y.-H. Deng, M.-C. Chen, L.-C. Peng, Y.-H. Luo, J. Qin, D. Wu, X. Ding, Y. Hu, et al., Science (2020).

Y. Wu, W.-S. Bao, S. Cao, F. Chen, M.-C. Chen, X. Chen, T.-H. Chung, H. Deng, Y. Du, D. Fan, et al., *Strong quantum computational advantage using a superconducting quantum processor* (2021).

I. Goodfellow, Y. Bengio, and A. Courville, *Deep Learning* (MIT Press, 2016), `http://www.deeplearningbook.org`.

D. Silver, A. Huang, C. J. Maddison, A. Guez, L. Sifre, G. van den Driessche, J. Schrittwieser, I. Antonoglou, V. Panneershelvam, M. Lanctot, et al., Nature **529**, 484 (2016).

D. Silver, J. Schrittwieser, K. Simonyan, I. Antonoglou, A. Huang, A. Guez, T. Hubert, L. Baker, M. Lai, A. Bolton, et al., Nature **550**, 354 (2017).

J. Biamonte, P. Wittek, N. Pancotti, P. Rebentrost, N. Wiebe, and S. Lloyd, Nature **549**, 195 (2017).

S. McArdle, S. Endo, A. Aspuru-Guzik, S. C. Benjamin, and X. Yuan, Rev. Mod. Phys. **92**, 015003 (2020).

I. Cong, S. Choi, and M. D. Lukin, Nature Physics **15**, 1273 (2019).

M. Henderson, S. Shakya, S. Pradhan, and T. Cook, *Quanvolutional neural networks: Powering image recognition with quantum circuits* (2019).

I. Kerenidis, J. Landman, and A. Prakash, in *International Conference on Learning Representations* (2020).

I. Kerenidis and A. Luongo, Phys. Rev. A **101**, 062327 (2020).

S. Oh, J. Choi, and J. Kim, in *2020 International Conference on Information and Communication Technology Convergence (ICTC)* (2020), pp. 236–239.

A. Pesah, M. Cerezo, S. Wang, T. Volkoff, A. T. Sornborger, and P. J. Coles, *Absence of barren plateaus in quantum convolutional neural networks* (2020).

S. Y.-C. Chen, T.-C. Wei, C. Zhang, H. Yu, and S. Yoo, *Quantum convolutional neural networks for high energy physics data analysis* (2020).

S. Wei, Y. Chen, Z. Zhou, and G. Long, *A quantum convolutional neural network on nisq devices* (2021).

J. Liu, K. H. Lim, K. L. Wood, W. Huang, C. Guo, and H.-L. Huang, *Hybrid quantum-classical convolutional neural networks* (2021).

S. Sim, P. D. Johnson, and A. Aspuru-Guzik, Advanced Quantum Technologies **2**, 1900070 (2019).

D. A. Meyer and N. R. Wallach, Journal of Mathematical Physics **43**, 4273 (2002).

D. P. Kingma and J. Ba, ArXiv e-prints (2014).

A Quantum circuits employed in the quantum convolutional layers

Four PQCs used in the Q-Conv are drawn in the Figure 6. They are extended to 9-qubit QC based on four PQCs suggested from Sim et al. (2019).

The effect of expressibility for higher entangling capability can be compared between two models QNN-2 and QNN-9, while the effect of entangling capability for similar expressibility can be compared between QNN-2, QNN-3 and QNN-10.

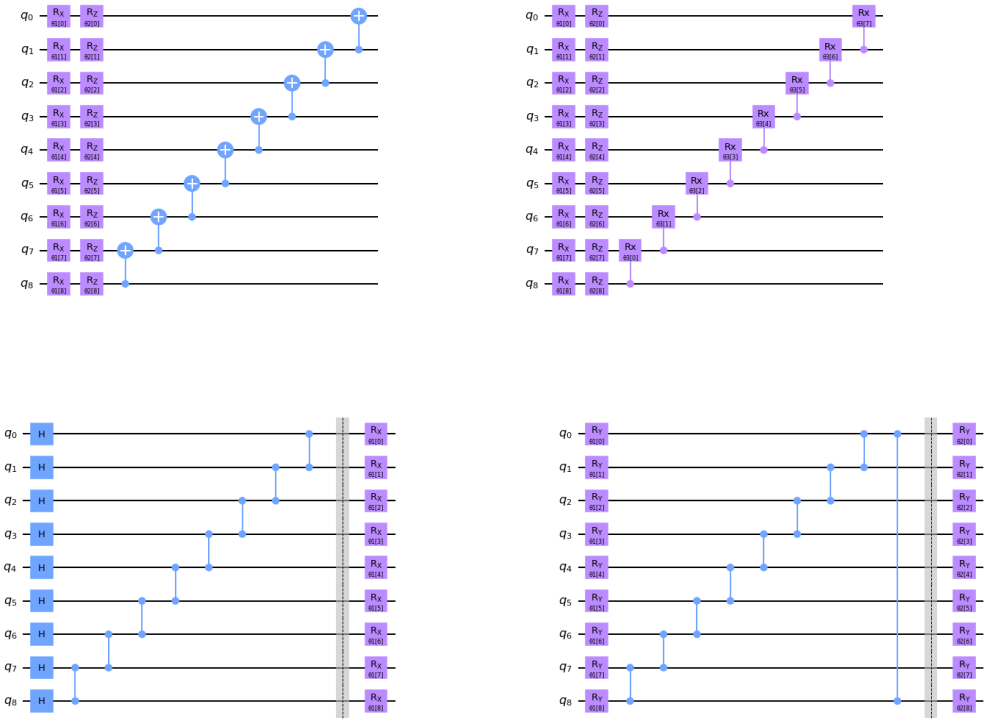

Figure 6: The quantum circuits employed in the qantum convolutional layer. QNN-2 (left top), QNN-3 (right top), QNN-9 (left bottom), and QNN-10 (right bottom).